Proceedings Paper:
Bahrani, S, Razavi, M and Salehi, JA (2016) Optimal Wavelength Allocation in Hybrid Quantum-Classical Networks. In: 24th European Signal Processing Conference (EUSIPCO 2016). EUSIPCO 2016, 29 Aug - 02 Sep 2016, Budapest, Hungary. IEEE , pp. 483-487. ISBN 978-0-9928-6265-7

https://doi.org/10.1109/EUSIPCO.2016.7760295

Optimal Wavelength Allocation in Hybrid Quantum-Classical Networks

Sima Bahrani[1], Mohsen Razavi[2], and Jawad A. Salehi[1]
[1]Electrical Engineering Department, Sharif University of Technology, Tehran, Iran.
[2]School of Electronic and Electrical Engineering, University of Leeds, Leeds, LS2 9JT, UK.

***Abstract*—An efficient method for optimal allocation of wavelengths in a hybrid dense-wavelength-division-multiplexing system, carrying both quantum and classical data, is proposed. The transmission of quantum bits alongside intense classical signals on the same fiber faces major challenges arising from the background noise generated by classical channels. Raman scattering, in particular, is shown to have detrimental effects on the performance of quantum key distribution systems. Here, by using a nearly optimal wavelength allocation technique, we minimize the Raman induced background noise on quantum channels, hence maximize the achievable secret key generation rate for quantum channels. It turns out the conventional solution that would involve splitting the spectrum into only two bands, one for quantum and one for classical channels, is only a suboptimal one. We show that, in our optimal arrangement, we might need several quantum and classical bands interspersed among each other.**

I. Introduction

Quantum key distribution (QKD) is a promising technology that offers unconditional security in applications with high security requirements. In the past three decades, there has been much progress in both theoretical and experimental aspects of QKD. Since the first experimental demonstration of QKD [1] up until now, QKD has seen considerable enhancement in reach and performance in point-to-point scenarios [2]. To further make QKD a cost-effective technology for large-scale applications, its adaptation to the infrastructure of existing classical communications networks is unavoidable [3], [4]. In particular, dense-wavelength-division-multiplexing (DWDM) techniques can enable the simultaneous transmission of both quantum and classical data on the same fiber. However, the transmission of quantum data alongside strong classical signals, in practice, faces some challenges due to nonlinear effects in fiber, such as Raman scattering and four-wave mixing [5], which may severely affect the operation of QKD links. Here, we consider a hybrid DWDM link with known numbers of quantum and classical channels and find a nearly optimal wavelength assignment method in the presence of Raman noise. Our proposed technique can be generalized to account for other sources of noise as well [6]. Raman noise has, however, been shown to be the dominant source of background noise in such hybrid setups [5].

The key problem in integrating quantum and classical communications channels is the background noise induced by classical channels onto quantum ones. Even if we allocate different wavelengths to the quantum and classical channels, as in DWDM, some of the noise generated by classical signals, especially the Raman noise, has non-zero components over a wide range of spectrum. Such a noise is not necessarily a major issue in conventional high-SNR classical communications systems, but it is a serious drawback to QKD systems, which often rely on single photons to carry information. In existing experiments that demonstrate the simultaneous operation of quantum and classical signals, various filtering schemes, in time and frequency, are used to reduce the effect of such a background noise [7], [8]. Such experiments, however, only consider very few classical/quantum channels. It is not clear, if we want to use the entire spectrum available in a DWDM link, how we should assign wavelengths to each of QKD and classical channels. Here, we propose an optimal wavelength allocation technique that maximizes the average key rate of a known number of QKD channels in the presence of a certain number of classical channels. We show that the optimal solution may involve grouping quantum and classical channels into multiple bands, interspersed among each other.

In the following, we first describe the problem in Sec. II, followed by its corresponding key-rate analysis in Sec. III. In Sec. IV, we describe our optimal wavelength allocation scheme followed by some numerical results in Sec. V, before concluding the paper in Sec. VI.

II. System Description

Consider the DWDM link shown in Fig. 1, where, consistent with the conventional notation in cryptography, the two nodes are denoted by Alice and Bob. We assume that there are a total of P channels, where M of which are to be allocated to QKD usage, while N forward and N backward channels will carry classical data. In Fig. 1, each QKD link uses efficient decoy-state BB84 protocol to generate secure keys [9]. The QKD signals are transmitted from Alice to Bob, while the classical data links can in general be bidirectional. Each classical channel is equipped with optical circulators to enable the transmission of signals in both directions on the same wavelength. We assume that the launch power of all data channels are chosen in such a way to guarantee a BER no more than 10^{-9}. For simplicity, here we have assumed that the laser power for all data channels is the same and is denoted by I.

The key problem we address here is to find the optimum wavelength assignment for specific values of N and M such that the sum of the secret key rates from our M QKD channels is maximized. We define the set $W = \{\lambda_1, \lambda_2, ..., \lambda_P\}$ as the set

of available wavelengths to be assigned to quantum and classical channels. The set of wavelengths assigned to forward classical, backward classical, and quantum channels, respectively, are denoted by $F = \{\lambda_{f_1}, \lambda_{f_2}, ..., \lambda_{f_N}\}$, $B = \{\lambda_{b_1}, \lambda_{b_2}, ..., \lambda_{b_N}\}$, and $Q = \{\lambda_{q_1}, \lambda_{q_2}, ..., \lambda_{q_M}\}$.

The key source of background noise considered in our analysis is the Raman-induced noise by classical channels onto quantum ones. Raman scattering arises from the inelastic scattering of photons and will introduce optical signals over a wide range of frequencies overlapping with the quantum channels [10]. We assume that data lasers with optical intensity I are used at the transmitter of the classical channels. The Raman noise power resulted from the data channel n, with wavelength $\lambda_{d_n} \in \{\lambda_{f_n}, \lambda_{b_n}\}$, received at the Bob's end of the QKD link m, with wavelength λ_{q_m}, for forward and backward scattering is, respectively, given by [5], [7]:

$$I^f_{nm} = Ie^{-\alpha L} L\Gamma(\lambda_{d_n}, \lambda_{q_m})\Delta\lambda, \tag{1}$$

$$I^b_{nm} = I\frac{(1-e^{-2\alpha L})}{2\alpha}\Gamma(\lambda_{d_n}, \lambda_{q_m})\Delta\lambda, \tag{2}$$

where α and L are, respectively, the fiber attenuation coefficient and the fiber length. Here, we have assumed equal fiber attenuation coefficients for quantum and classical channels [11]. In the above equations, $\Gamma(\lambda_{d_n}, \lambda_{q_m})$ is the Raman cross section (per fiber length and bandwidth) and $\Delta\lambda$ denotes the bandwidth of the quantum receiver. Figure 2 shows measured Raman cross section, $\rho(\lambda)$, for a pump laser centered at 1550 nm in a standard single mode fiber [5]. To obtain $\Gamma(\lambda_{d_n}, \lambda_{q_m})$, we assume that the Raman spectrum for a classical signal at wavelength λ_{d_n} would be a shifted version of the spectrum shown in Fig. 2. That is, $\Gamma(\lambda_{d_n}, \lambda_{q_m}) = \rho(\lambda_1)$, where the wavelength λ_1 corresponds to the Raman frequency shift $\Delta_f = c/\lambda_{q_m} - c/\lambda_{d_n}$, where c is the speed of light, given by

$$\lambda_1 = (\frac{1}{\lambda_{q_m}} - \frac{1}{\lambda_{d_n}} + \frac{1}{1550})^{-1} \quad \text{(nm)}. \tag{3}$$

The Raman induced photon count probability at the detectors of the mth quantum receiver, for forward and backward channels can, respectively, be expressed as

$$p^f_{nm} = I^f_{nm}\lambda_{q_m}T_d\eta_d/(2hc) = \gamma^f\lambda_{q_m}\Gamma(\lambda_{d_n}, \lambda_{q_m}), \tag{4}$$

$$p^b_{nm} = I^b_{nm}\lambda_{q_m}T_d\eta_d/(2hc) = \gamma^b\lambda_{q_m}\Gamma(\lambda_{d_n}, \lambda_{q_m}), \tag{5}$$

where γ^f and γ^b are given by

$$\gamma^f = Ie^{-\alpha L}L\Delta\lambda T_d\eta_d/(2hc), \tag{6}$$

$$\gamma^b = I\frac{(1-e^{-2\alpha L})}{2\alpha}\Delta\lambda T_d\eta_d/(2hc). \tag{7}$$

Here, h is the Planck's constant, η_d denotes the quantum efficiency, and T_d is the gate width of the QKD receiver photodetectors. The factor $1/2$ reflects the fact that the background noise would be split between two orthogonal polarizations at the QKD receiver. Note that, in (6) and (7), the right-hand side is wavelength independent.

There are several methods proposed in the literature to mitigate the effect of the Raman crosstalk. Effective filtering in both frequency and time domains at quantum receivers can significantly suppress the Raman noise. Another approach is to reduce the launch power of data lasers, I, to the value that matches the receiver sensitivity [7], [8]. In this paper, we assume that such conventional noise reduction methods are in place. For more advanced setups, one can consider orthogonal frequency division multiplexing techniques, which, in principle, can limit the background noise to only one time-frequency mode [12], [13].

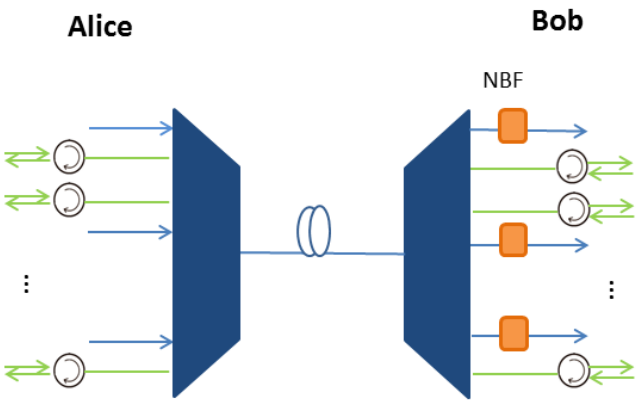

Fig. 1: The hybrid quantum-classical DWDM system structure. The classical channels (green) are equipped with circulators to enable bidirectional transmission. The quantum channels (blue) provide secure communications from Alice to Bob. NBF denotes narrow bandpass filter.

III. Key Rate Analysis

In this section, we examine the performance of the quantum channels in the proposed DWDM system in more detail. We consider a single QKD channel and investigate its operation in the presence of multiple classical channels. Denoting the average number of photons for the main signal state, in the employed decoy-state protocol, by μ, the secret key rate per transmitted pulse in the QKD channel, at the limit of an infinitely long key, is lower bounded by $\max[0, P(\mathrm{Y}_0)]$, where [14]

$$P(\mathrm{Y}_0) = Q_1(1 - h(e_1)) - fQ_\mu h(E_\mu). \tag{8}$$

Here, $h(p) = -p\log_2 p - (1-p)\log_2(1-p)$ is the binary entropy function and f denotes the error correction inefficiency. In the above equation, Q_μ, E_μ, Q_1, and e_1 represent the overall gain, the quantum bit error rate (QBER), the gain of the single photon state, and the error rate of the single photon state, respectively. The overall gain, Q_μ, and the QBER, E_μ, are respectively given by

$$\begin{aligned} Q_\mu &= 1 - (1 - \mathrm{Y}_0)e^{-\eta\mu}, \\ E_\mu &= (\mathrm{Y}_0/2 + e_d(1 - e^{-\eta\mu}))/Q_\mu, \end{aligned} \tag{9}$$

while the gain and the error rate of the single photon state are, respectively, as follows:

$$\begin{aligned} Q_1 &= \mathrm{Y}_1\mu e^{-\mu}, \\ e_1 &= (\mathrm{Y}_0/2 + e_d\eta)/\mathrm{Y}_1. \end{aligned} \tag{10}$$

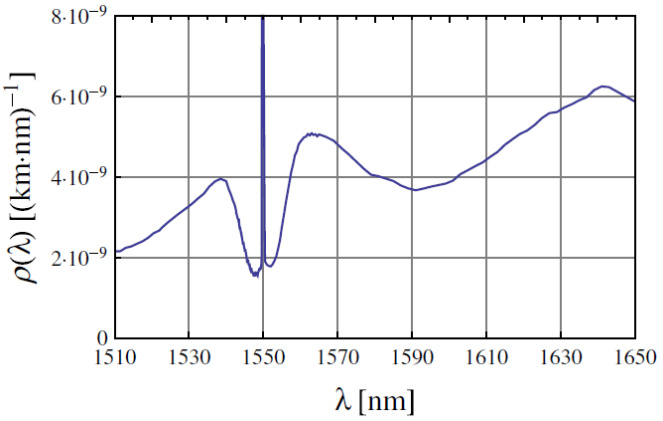

Fig. 2: Measured Raman cross section for a pump laser centered at 1550 nm in a standard single mode fiber as reported in [5].

Here, Y_0 represents the probability of having detector clicks at the Bob's end without transmitting any photons, and Y_1 is the yield of a single-photon state. Furthermore, the parameters e_d and η denote the misalignment probability and the total transmissivity of the link, respectively. With the repetition period of the QKD signal denoted by T_s, the secret key rate of the m^{th} QKD channel is given by

$$R_m = \max[0, P(Y_0)/T_s], \tag{11}$$

where

$$Y_0 = 1 - (1 - (p_{\rm dc} + p_m))^2. \tag{12}$$

In the above equation, $p_{\rm dc} = \gamma_{\rm dc} T_d$, where $\gamma_{\rm dc}$ denotes the photodetectors dark count rate and p_m denotes the total Raman photon count probability per QKD detector, given by

$$p_m = \gamma^b \sum_{n=1}^{N} \lambda_{q_m} \rho^b_{nm} + \gamma^f \sum_{n=1}^{N} \lambda_{q_m} \rho^f_{nm}, \tag{13}$$

where, from (4) and (5), $\rho^f_{nm} = \Gamma(\lambda_{f_n}, \lambda_{q_m})$ and $\rho^b_{nm} = \Gamma(\lambda_{b_n}, \lambda_{q_m})$, respectively, represent the Raman cross section noise for the n^{th} forward and backward channels.

IV. Optimal Wavelength Assignment

The key rate analysis presented in the previous section indicates that the operation of QKD channels in the DWDM system in Fig. 1 is highly dependent on the number of classical (and quantum) channels, as well as their location in the wavelength grid. A proper wavelength assignment method is, therefore, of significant importance in this hybrid DWDM system. In this section, we propose an optimal wavelength assignment method that maximizes the overall key rate of QKD channels. We will then compare the optimal solution with what conventionally may seem to be the best option, as explained next.

The form of the Raman cross section in Fig. 2 may imply that the best strategy for allocating wavelengths to QKD channels is to locate them on the left-hand side of the classical ones [11]. That is, given that the noise in the anti-Stokes region of Fig. 2 is seemingly lower than that of the Stokes region, it may make sense if we allocate the higher wavelengths to classical channels, and the lower ones to quantum channels. It turns out, however, that this technique is only a suboptimal solution, and the optimum wavelength allocation scheme intersperses classical and quantum channels.

In our optimization problem, we look for sets of wavelengths, F, B, and Q, such that the total key rate is maximized. In this case the maximum key rate is given by

$$MR_{\rm avg} = \max_{F,B,Q\subset W} \sum_{m=1}^{M} R_m, \tag{14}$$

where $R_{\rm avg}$ is the average key rate obtained from our M QKD channels. In order to simplify the above formulation, we investigate the dependence of the secret key rate on Raman photon count probabilities. Based on the key rate analysis presented in Sec. III, by increasing Raman photon count probability the generated secret key rate would drop. As an example, Fig. 3 shows the secret key rate of a single QKD channel as a function of Raman photon count probability, at a fiber length of 50 km. The QKD system parameters are explained in Sec. V and shown in Table I. As expected, the rate is a descending function of the background noise. Moreover, within the regime of interest, we can fit a line to this curve without losing much accuracy. We can then approximate the optimization criterion in (14) with the following

$$\min_{F,B,Q\subset W} \sum_{m=1}^{M} p_m, \tag{15}$$

which is linear in p_m. The above approximation will, in principle, provide us with a near-optimal solution to the optimization criterion in (14). Our simulation results, however, show that this approximation provides us with the optimum solutions for the wavelength assignment cases considered in Sec. V. It also substantially reduces the complexity of the optimization problem. Using (6) and (7), (15) can be written as

$$\min_{F,B,Q\subset W} \gamma^b \{\sum_{n=1}^{N} (\sum_{m=1}^{M} \lambda_{q_m} \rho^b_{nm})\} + \gamma^f \{\sum_{n=1}^{N} (\sum_{m=1}^{M} \lambda_{q_m} \rho^f_{nm})\}. \tag{16}$$

Since γ^b and γ^f are wavelength independent, we should minimize the terms in the brackets. It can be shown that both terms are minimized over the same sets of wavelengths. Therefore, we can conclude that, for optimal wavelength assignment, all classical channels should essentially be bidirectional, i.e, $\lambda_{f_n} = \lambda_{b_n}$, for $n = 1, ..., N$. In this case, (16) reduces to finding

$$\min_{B,Q\subset W} \sum_{n=1}^{N} (\sum_{m=1}^{M} \lambda_{q_m} \rho_{nm}), \tag{17}$$

where $\rho_{nm} = \rho^b_{nm} = \rho^f_{nm}$.

The optimum wavelength assignment is obtained by solving the optimization problem in (17). To start, we define a $P \times P$ matrix, $\mathbf{D}$, with elements given by

$$\mathbf{D}_{nm} = \begin{cases} \lambda_{q_m} \rho_{nm} & n \neq m \\ \infty & n = m \end{cases}. \tag{18}$$

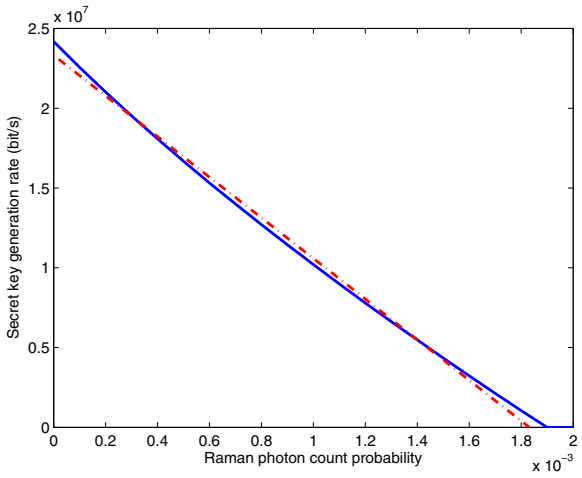

Fig. 3: Secret key generation rate versus Raman photon count probability (blue solid curve) and its linear approximation (red dash-dotted curve).

TABLE I: Nominal values used for QKD system parameters.

Parameter	Value
Average number of photons per signal pulse, μ	0.48
Quantum Efficiency	0.3
Receiver dark count rate, γ_{dc}	1E-7 ns^{-1}
Error correction inefficiency, f	1.16
Misalignment probability, e_d	0.015
Laser pulse repetition interval, T_s	250 ps
Time gate interval, T_d	100 ps

According to (18), our problem can be formulated as finding N rows and M columns of matrix $\mathbf{D}$ such that the summation of elements on the intersection of these rows and columns is minimum (the diagonal elements of $\mathbf{D}$ is excluded). This is equivalent to finding an assignment for classical and quantum channels that minimizes the overall background noise on quantum ones. In order to find the optimum solution, we have to consider different combinations of N rows out of P (or M columns out of P) and investigate $\binom{P}{N}$ (or $\binom{P}{M}$, whichever is smaller) cases. The total number of cases to search through is $min\{\binom{P}{N}, \binom{P}{M}\}$. In each case, the corresponding rows (or columns) of $\mathbf{D}$ are added. Then, the M columns (or N rows) with the smallest summation is chosen. In the end, the case with the smallest total summation is determined as the optimum solution.

Note that the optimization problem in (17) is also applicable in a unidirectional scenario. For instance, in dual-fiber DWDM systems, since backward Raman scattering is stronger than the forward one, it is reasonable to multiplex the quantum channels with the forward data signals on the same fiber. In this case, the optimum wavelength assignment pattern can be obtained by the above proposed method.

V. Numerical Results

In this section, we provide numerical examples for the proposed wavelength assignment method. We consider a DWDM system with 200 GHz channel spacing with the wavelength set $W = \{1530.8\text{ nm}, 1532.4\text{ nm}, ..., 1564.4\text{ nm}\}$ in the C-band.

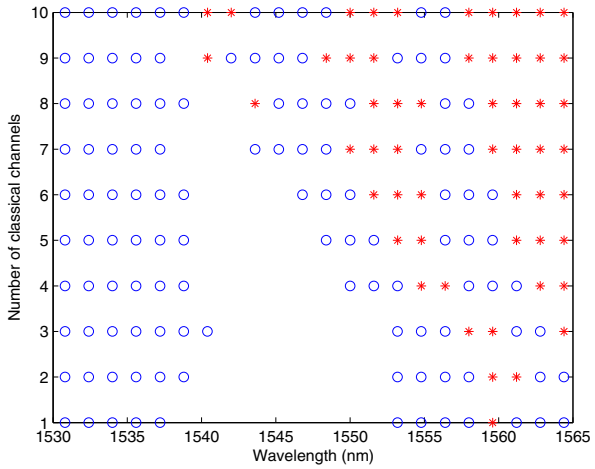

Fig. 4: Optimum wavelength assignment patterns for $M = 12$ in a hybrid DWDM system with 200-GHz channel spacing. Each row depicts the optimum location of quantum and classical channels in the wavelength grid, where $*$ represents a classical channel and $\circ$ represents a quantum one.

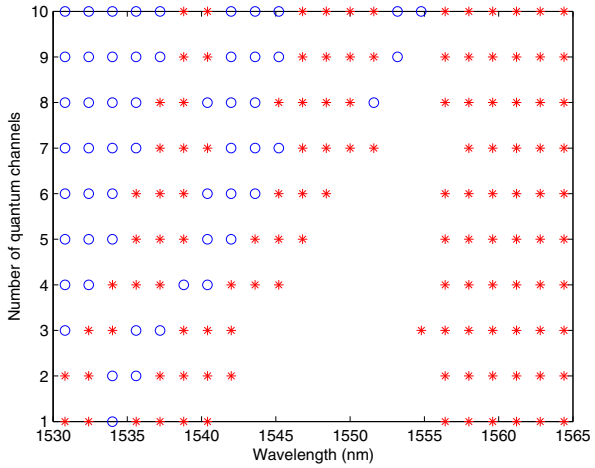

Fig. 5: Optimum wavelength assignment patterns for $N = 12$ in a hybrid DWDM system with 200-GHz channel spacing. Each row depicts the optimum location of quantum and classical channels in the wavelength grid.

We use the numerical values reported in relevant experiments for our system parameters. For the QKD channels, these values are summarized in Table I. For the classical channels, we assume that on-off-keying signaling with a data rate of 1 GHz is used. The launch power of data lasers are set to $I = 10^{(-3.5+\alpha L/10)}$ mW, which corresponds to -35 dBm receiver sensitivity, corresponding to a $BER < 10^{-9}$ [7]. The fiber attenuation coefficient, α is assumed to be $\alpha = 0.2$ dB/km. At QKD receivers, optical filters with 15 GHz of bandwidth are used [8]. The effective time gate of detectors is 100 ps [7].

Figure 4 shows the optimum wavelength assignment for $M = 12$ quantum channels and different values of classical channels, N. In this figure, "$*$" and "$\circ$", respectively, denote the location of classical and quantum channels on the grid. For instance, at $N = 5$, the optimum allocation assigns the

first six channels to QKD users, the following five channels remain unused, while the next three channels are quantum again. The first batch of classical channels will then follow the previous three quantum channels, followed by another three quantum and three classical channels. As can be seen, the optimum pattern for each N is, in general, not compatible with the conventional method of having two separate quantum and classical bands in the wavelength grid. For example in Fig. 4, for $N \leq 2$, there are four bands, where three of them are allocated to quantum channels, and the classical band is surrounded by quantum bands. As N increases, the optimum wavelength pattern may include more interleaved quantum and classical bands. For $3 \leq N \leq 7$, we have two classical and three quantum bands. For $N \geq 8$, the number of bands reaches its maximum of six. In none of the cases considered in this example, the optimum wavelength pattern is compatible with the conventional suboptimal method of two separate quantum and classical bands.

Figure 5 shows the optimum wavelength assignment for $N = 12$ classical channels and different values of quantum channels, M. It can be seen that there is a duality between almost all the patterns in this figure and that of Fig. 4. In both cases, the optimally allocated wavelengths create a pattern similar to the Raman cross section in Fig. 2. This is in line with the fact that the only source of background noise considered in our analysis is the Raman-induced noise. In the presence of other sources of noise, one can extend the optimal wavelength allocation technique developed in Sec. IV to obtain the optimal assignment. For instance, one may need to leave an unused channel between quantum and classical sub-bands in Figs. 4 and 5 if one considers the high power leakage from classical channels to their immediate adjacent channels [8].

Finally, we compare our proposed optimum wavelength assignment with the conventional method that assigns the highest and lowest wavelengths in the wavelength grid, respectively, to the classical and quantum bands. Figure 6 depicts the average secret key generation rate for $M = 6$ at a fiber length of 90 km. It is clear that our optimum wavelength assignment enhances the average key rate. For example, for $N = 12$ classical channels, we achieve about 70% increase in the key rate by using our optimum wavelength assignment technique.

VI. Conclusions

In this paper, we examined the optimum wavelength allocation in an integrated quantum-classical network. We showed that the conventional solution of assigning two separate bands to quantum and classical channels would not necessarily be the optimal solution. We further investigated the optimum wavelength allocation patterns. Our results showed that these patterns could include multiple quantum and classical bands. Moreover, we showed that, by using our proposed optimal assignment technique, the achievable secret key generation rates in QKD channels could be improved.

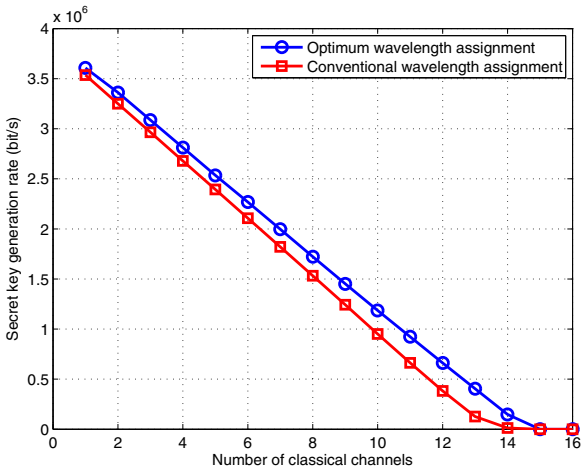

Fig. 6: The average secret key generation rate, R_{avg}, for optimum and conventional wavelength assignment methods for different numbers of classical channels at $M = 6$ and $L = 90$ km.

References

[1] C. H. Bennett, F. Bessette, G. Brassard, L. Salvail, and J. Smolin, "Experimental quantum cryptography," *Journal of cryptology*, vol. 5, no. 1, pp. 3–28, 1992.

[2] V. Scarani, H. Bechmann-Pasquinucci, N. J. Cerf, M. Dušek, N. Lütkenhaus, and M. Peev, "The security of practical quantum key distribution," *Rev. Mod. Phys.*, vol. 81, no. 3, pp. 1301–1350, Sep 2009.

[3] N. A. Peters, P. Toliver, T. E. Chapuran, R. J. Runser, S. R. McNown, C. G. Peterson, D. Rosenberg, N. Dallmann, R. J. Hughes, K. P. McCabe, J. E. Nordholt, and K. T. Tyagi, "Dense wavelength multiplexing of 1550nm QKD with strong classical channels in reconfigurable networking environments," *New J. Phys.*, vol. 11, p. 045012, April 2009.

[4] T. E. Chapuran, P. Toliver, N. A. Peters, J. Jackel, M. S. Goodman, R. J. Runser, S. R. McNown, N. Dallmann, R. J. Hughes, K. P. McCabe, J. E. Nordholt, C. G. Peterson, K. T. Tyagi, L. Mercer, and H. Dardy, "Optical networking for quantum key distribution and quantum communications," *New J. Phys.*, vol. 11, p. 105001, Oct. 2009.

[5] P. Eraerds, N. Walenta, M. Legre, N. Gisin, and H. Zbinden, "Quantum key distribution and 1 gbps data encryption over a single fibre," *New Journal of Physics*, vol. 12, no. 6, p. 063027, 2010.

[6] S. Bahrani, M. Razavi, and J. A. Salehi, "Crosstalk reduction in hybrid quantum-classical networks," 2016, submitted to Scientia Iranica.

[7] K. Patel, J. Dynes, I. Choi, A. Sharpe, A. Dixon, Z. Yuan, R. Penty, and A. Shields, "Coexistence of high-bit-rate quantum key distribution and data on optical fiber," *Physical Review X*, vol. 2, no. 4, p. 041010, 2012.

[8] K. Patel, J. Dynes, M. Lucamarini, I. Choi, A. Sharpe, Z. Yuan, R. Penty, and A. Shields, "Quantum key distribution for 10 gb/s dense wavelength division multiplexing networks," *Applied Physics Letters*, vol. 104, no. 5, p. 051123, 2014.

[9] H.-K. Lo, H.-F. Chau, and M. Ardehali, "Efficient quantum key distribution scheme and a proof of its unconditional security," *Journal of Cryptology*, vol. 18, no. 2, pp. 133–165, 2005.

[10] G. P. Agrawal, *Nonlinear fiber optics*. Academic press, 2007.

[11] R. Kumar, H. Qin, and R. Alléaume, "Coexistence of continuous variable QKD with intense DWDM classical channels," *New Journal of Physics*, vol. 17, no. 4, p. 043027, 2015.

[12] S. Bahrani, M. Razavi, and J. Salehi, "Orthogonal frequency-division multiplexed quantum key distribution," *Lightwave Technology, Journal of*, vol. 33, no. 23, pp. 4687–4698, Dec. 2015.

[13] S. Bahrani, M. Razavi, and J. A. Salehi, "Orthogonal frequency division multiplexed quantum key distribution in the presence of Raman noise," in *Proc. SPIE*, vol. 9900, 2016, pp. 99 001C–99 001C–7.

[14] M. Razavi, "Multiple-access quantum key distribution networks," *IEEE Trans. Commun.*, vol. 60, no. 10, pp. 3071–3079, 2012.